

Magnetoresistance peculiarities of $\text{Bi}_{95.69}\text{Mn}_{3.69}\text{Fe}_{0.62}$ in magnetic fields up to 140 kOe

A. V. Terekhov¹, K. Rogacki², V. M. Yarovyi¹, V. B. Stepanov¹, Yu. A. Kolesnichenko¹,
A. D. Shevchenko³, Z. D. Kovalyuk⁴, E. Lähderanta⁵, and A. L. Solovjov^{1,2,5}

¹*B. Verkin Institute for Low Temperature Physics and Engineering of the National Academy of Science of Ukraine, Kharkiv 61103, Ukraine*

E-mail: terekhov@ilt.kharkov.ua, terekhov.andrii@gmail.com

²*Institute of Low Temperature and Structure Research, Polish Academy of Sciences
50-422 Wrocław, Poland*

³*G. V. Kurdyumov Institute for Metal Physics of the National Academy of Science of Ukraine
Kyiv 03142, Ukraine*

⁴*I. M. Frantsevich Institute for Problems of Material Science of the National Academy of Science of Ukraine
Chernivtsi 58001, Ukraine*

⁵*Lappeenranta University of Technology, School of Engineering Science, 53850 Lappeenranta, Finland*

Received April 24, 2023, published online June 22, 2023

The magnetic-field dependences of the electrical resistivity $\Delta\rho/\rho_0(H)$ of the textured polycrystal $\text{Bi}_{95.69}\text{Mn}_{3.69}\text{Fe}_{0.62}$ have been studied for the first time, for the $\mathbf{H} \perp \mathbf{I}$ and $\mathbf{H} \parallel \mathbf{I}$ configurations at temperatures 5, 80, 150, and 300 K. It has been established that the $\Delta\rho/\rho_0(H)$ dependences significantly differ from those obtained for pure bismuth due to the influence of the internal magnetism of the α -BiMn phase inclusions on the behavior of charge carriers in the bismuth matrix. The maxima of $\Delta\rho/\rho_0(H)$ at $H \approx 30$ and ≈ 40 kOe have been found, for the longitudinal and transverse magnetoresistance, respectively. These maxima may be related to reaching the quantum limit in the material we have studied.

Keywords: magnetic-field dependences of electrical resistance, textured polycrystal, α -BiMn phase, bismuth, quantum limit.

Introduction

A large number of unusual physical properties of bismuth have attracted interest in its comprehensive study for more than 100 years. The following effects were experimentally observed in bismuth: the Shubnikov–de Haas and de Haas–van Alphen effects, large positive magnetoresistance, cyclotron resonance in the metal, oscillating magnetostriction, magneto-plasma waves, and a number of size effects, all for the first time in Refs. 1, 2. For many years it was believed that bulk bismuth does not pass into the superconducting state. However, recently, a group of Indian scientists discovered such a transition in single crystal bismuth at ultra low temperatures ($T_c \approx 0.5$ mK) [3].

Meanwhile, compounds with bismuth are also of great interest to scientists working in solid state physics. Thus, $\text{Bi}_2\text{Sr}_2\text{Ca}_2\text{Cu}_3\text{O}_{10+x}$ (BiSCCO, Bi-2223) is a high-temperature

superconductor with a transition temperature T_c to the superconducting state of about 110 K [4], an alloy of 88% Bi and 12% Sb exhibits anomalous magnetoresistance effect [5], $\text{Bi}_{0.9}\text{Sb}_{0.1}$ is strongly spin-orbit coupled insulator with an odd number of Dirac points and a negative Z_2 topological Hall phase [6], 3D Dirac fermions with linear dispersions along all momentum directions and properties related with it had been discovered in Na_3Bi [7], and, finally, it is worth mentioning BiMn solid solutions, which occupy a special place among permanent magnets [8, 9]. BiMn is a ferromagnet with magnetic ordering at ≈ 640 K and a high coercive force value at room temperature that is close to the values in permanent magnets based on rare-earth elements [8, 9]. This, as well as the low cost of this material compared to rare-earth magnets, makes it attractive for practical use in high-temperature applications.

Despite of the huge number of works deal with the study of the magnetic properties of BiMn solid solutions, there have been almost no studies of the behavior of electric transport in them. Such studies are certainly important both in fundamental and applied aspects. Firstly, these materials contain a large amount of Bi and therefore it is quite likely that there is a large increase in electrical resistance in a magnetic field (positive magnetoresistance), which also occurs in pure bismuth. In addition, as noted above, BiMn is a fairly strong magnet, so it is interesting to study the effect of internal magnetism on electrical resistance.

A few years ago, our group studied electrical transport in the $\text{Bi}_{95.69}\text{Mn}_{3.69}\text{Fe}_{0.62}$ material [10, 11]. It was found that in a magnetic field, the temperature dependence of the electrical resistance of this material behaves in a non-monotonic manner, and the magnetoresistance is positive in the entire temperature range used and can reach several thousand percent in a magnetic field up to 140 kOe. A strong anisotropy of the electrical resistance was also found in the measurements performed in the magnetic field and for different crystallographic directions. It was assumed that the anomalous behavior of the temperature dependence of the electrical resistance in $\text{Bi}_{95.69}\text{Mn}_{3.69}\text{Fe}_{0.62}$ compared to pure bismuth is associated with a change in the degree of overlapping between the electron and hole regions of the Fermi surface under the influence of both internal magnetism and an external magnetic field. At the same time, the mechanisms for the appearance of specific temperature dependences of magnetoresistance have not yet been clearly identified. In addition, the magnetic-field dependences of the magnetoresistance have not yet been investigated in this material either.

The aim of this work is the study of the magnetic-field dependences of the electrical resistance of $\text{Bi}_{95.69}\text{Mn}_{3.69}\text{Fe}_{0.62}$. This may shed light on the mechanisms of the unusual behavior of the magnetoresistance in this material. Thanks to this, it will be possible to create not only permanent magnets with high coercive force values, but also materials with high magnetoresistance values based on BiMn solid solutions, which is important when using them as magnetic field sensors and digital data storage devices.

Samples and experimental method

The starting materials for the samples were bismuth and manganese with a purity of $> 99.999\%$. Synthesis and crystal growth were carried out in graphitized quartz ampules with a diameter of 16–18 mm, evacuated to a residual pressure of $\approx 10^{-2}$ Pa. The samples were obtained by Bridgeman crystallization at the temperature of 630 K with the growth rate of 1.5 mm/h. Under such growth conditions, production of single crystal and coarse-grain textured samples is possible. To grow quality materials (especially at the crystallization front), it is necessary to stabilize the furnace temperature. This was accomplished by using a RIF-101 temperature control unit with an accuracy of $\pm 0.5^\circ\text{C}$.

Finished ingots had cylindrical shape. To measure the electrical resistance, parallelepiped-shaped specimens with dimensions of approximately $7 \times 2 \times 2$ mm were cut along the base of the cylinder which conventionally is perpendicular to the c axis.

A detailed structural study of this material was carried out and reported in Ref. 11. It is shown that $\text{Bi}_{95.69}\text{Mn}_{3.69}\text{Fe}_{0.62}$ is a textured polycrystal and is in fact a bismuth matrix with inclusions of the α -BiMn magnetic phase. It was also shown that iron does not form intermetallic phases with bismuth. Therefore, it is assumed that small amounts of individual iron inclusions present in our compound do not have a decisive effect on the electrical and magnetic properties of this material.

The magnetoresistance measurements were performed using a standard four-probe circuit on automated setup (PPMS) from Quantum Design. Current and potential contacts were made with silver paste. Resistivity measurements were carried out in alternating current mode ($I = 30$ mA, $f = 17$ Hz) with current directed along the larger dimension of the sample. The measurements were made for the following mutual directions of the field and current: $\mathbf{H} \perp \mathbf{I}$ and $\mathbf{H} \parallel \mathbf{I}$. Magnetic field sweep was performed from -140 to 140 kOe at temperatures of 5, 80, 150, and 300 K. For these measurements, the constant magnetic field was supplied by a superconducting solenoid.

Results and discussion

Magnetoresistance for $\mathbf{H} \perp \mathbf{I}$ configuration

Figure 1 shows the magnetic-field dependences of the magnetoresistance of $\text{Bi}_{95.69}\text{Mn}_{3.69}\text{Fe}_{0.62}$ plotted in relative units $\Delta\rho/\rho_0 = (\rho_H - \rho_0)/\rho_0 \cdot 100\%$ at fixed temperatures of 5, 80, 150, and 300 K for the configuration $\mathbf{H} \perp \mathbf{I}$. Measurements were taken with field directed up and down ($0 \rightarrow 150$ kOe, $150 \rightarrow 0$ kOe, $0 \rightarrow -150$ kOe, $-150 \rightarrow 0$ kOe). The obtained curves were quite symmetrical.

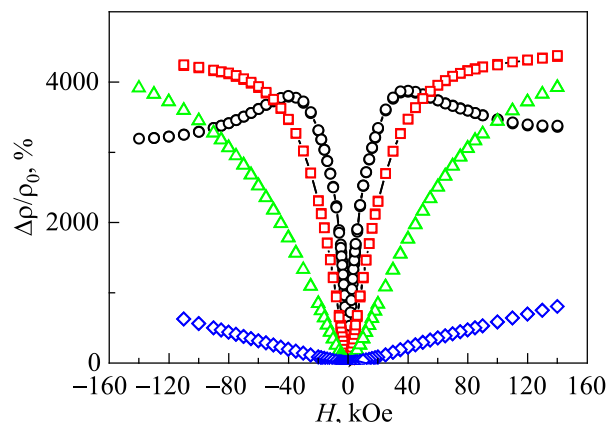


Fig. 1. (Color online) Magnetic-field dependences of the magnetoresistance $\Delta\rho/\rho_0 = (\rho_H - \rho_0)/\rho_0 \cdot 100\%$ of $\text{Bi}_{95.69}\text{Mn}_{3.69}\text{Fe}_{0.62}$ measured for the $\mathbf{H} \perp \mathbf{I}$ at fixed temperatures, K: 5 (\circ), 80 (\square), 150 (\triangle), and 300 (\diamond).

There were no hysteresis phenomena in the magnetic-field dependences of $\Delta\rho/\rho_0$. The maximum magnetoresistance value was observed at 80 K, $\Delta\rho/\rho_0 \approx 4380\%$ in a field of 140 kOe. It is very likely that at this temperature the magnetoresistance in fields above 140 kOe can reach saturation. Magnetoresistance is positive at all temperatures. The increasing rate in magnetoresistance with the magnetic field increasing is the largest at the lowest temperatures.

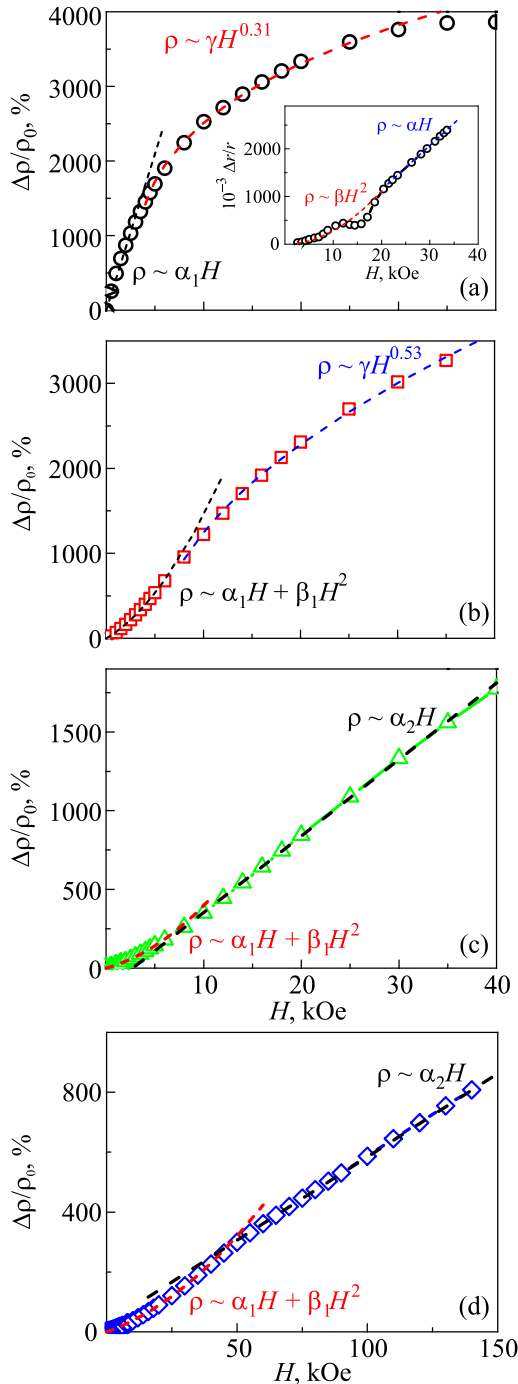


Fig. 2. (Color online) Magnetic-field dependences of the magnetoresistance $\Delta\rho/\rho_0 = (\rho_H - \rho_0)/\rho_0 \cdot 100\%$ of $\text{Bi}_{95.69}\text{Mn}_{3.69}\text{Fe}_{0.62}$ for the $\mathbf{H} \perp \mathbf{I}$ at several fixed temperatures, K: 5 (a), 80 (b), 150 (c), and 300 (d). Inset in Fig. 2(a) shows the literature data for pure bismuth [12] in the same range of magnetic fields.

The magnetoresistance increases monotonically with the field increasing at temperatures of 80, 150, and 300 K. At 5 K, the magnetoresistance first increases rapidly, reaching a maximum at 40 kOe, and then begins to decrease.

Figure 2(a) shows the field dependences of the magnetoresistance of our sample for $\mathbf{H} \perp \mathbf{I}$ configuration and pure bismuth [Inset in Fig. 2(a)] at $T = 5$ K [12]. This comparison is reasonable because our sample is a bismuth matrix with α -BiMn magnetic phase inclusions and the conductivity is due to current flowing through the bismuth matrix, which is influenced by α -BiMn magnetic phase uniformly distributed over the sample volume. Figure 2(a) shows that the field dependences of the magnetoresistance for pure bismuth and our sample are very different. There is a quadratic field dependence of magnetoresistance $\Delta\rho/\rho_0 \sim H^2$ in field interval 0–12 kOe which changes to linear above 12 kOe in pure bismuth [12–14]. A quadratic dependence and a linear dependence are observed in bismuth up to room temperature [13, 15]. As can be seen in Fig. 2(a) the quadratic dependence of $\Delta\rho/\rho_0 \sim H^2$ in the case of $\text{Bi}_{95.69}\text{Mn}_{3.69}\text{Fe}_{0.62}$ is not observed. The $\Delta\rho/\rho_0(H)$ up to about 5 kOe is linear, and above that there is a power dependence $\Delta\rho/\rho_0 \sim H^{0.31}$. At 80 K [Fig. 2(b)] $\Delta\rho/\rho_0 \sim \alpha_1 H + \beta_1 H^2$ in weak magnetic field and above 7 kOe a power dependence $\Delta\rho/\rho_0 \sim H^{0.53}$ with a larger power index than at $T = 5$ K is observed. The $\Delta\rho/\rho_0(H)$ dependences of $\text{Bi}_{95.69}\text{Mn}_{3.69}\text{Fe}_{0.62}$ at temperatures of 150 and 300 K [Figs. 2(c) and 2(d)] essentially differ from those at the liquid helium temperature. As the field increases, the dependence $\Delta\rho/\rho_0 \sim \alpha_1 H + \beta_1 H^2$ is first observed, which changes to a linear one at higher fields.

The interval where $\rho/\rho_0 \sim \alpha_1 H + \beta_1 H^2$ becomes larger with increasing temperature (0–10 kOe for 150 K and 0–50 kOe for 300 K).

Magnetoresistance for $\mathbf{H} \parallel \mathbf{I}$ configuration

Figure 3 shows the magnetic-field dependences of magnetoresistance plotted in relative units $\Delta\rho/\rho_0 = (\rho_H - \rho_0)/\rho_0 \cdot 100\%$, which measured at fixed temperatures of 5, 80, 150, and 300 K, for the $\mathbf{H} \parallel \mathbf{I}$ configuration. The curves are quite symmetrical, and no hysteresis phenomena are observed. The maximum value of magnetoresistance was observed at 150 K, $\Delta\rho/\rho_0 \approx 860\%$ in 140 kOe. The dependence $\Delta\rho/\rho_0(H)$ does not reach saturation at higher magnetic fields. Interestingly, the maximum magnetoresistance value is 5 times lower than for the $\mathbf{H} \perp \mathbf{I}$ configuration and is observed at higher temperatures. Magnetoresistance is positive at all temperatures. As for the $\mathbf{H} \perp \mathbf{I}$ configuration, the rate of increase in magnetoresistance with increasing magnetic field is for $\mathbf{H} \parallel \mathbf{I}$ maximal at low temperatures. At temperatures of 80, 150, and 300 K, the magnetoresistance increases monotonically as the field grows up. However, at 5 K, the magnetoresistance first increases rapidly, reaching a maximum at 30 kOe, and then begins to decrease. Accordingly,

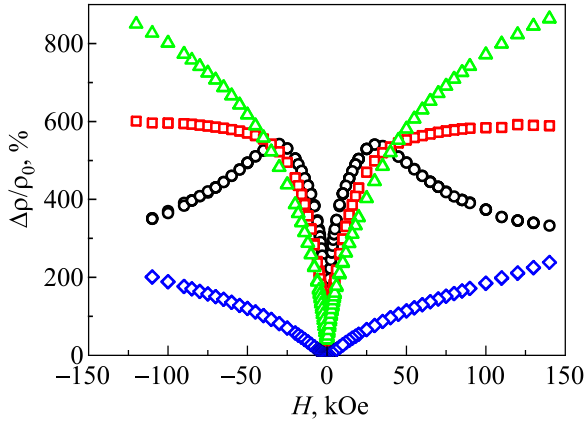


Fig. 3. (Color online) Magnetic-field dependences of the magnetoresistance $\Delta\rho/\rho_0 = (\rho_H - \rho_0)/\rho_0 \cdot 100\%$ of $\text{Bi}_{95.69}\text{Mn}_{3.69}\text{Fe}_{0.62}$ measured for $\mathbf{H} \parallel \mathbf{I}$ at fixed temperatures, K: 5 (\circ), 80 (\square), 150 (\triangle), and 300 (\diamond).

at 80 K the magnetoresistance first increases as the field grows up, and then goes to saturation above 50 kOe.

Figure 4 shows the field dependences of the magnetoresistance of the $\text{Bi}_{95.69}\text{Mn}_{3.69}\text{Fe}_{0.62}$ sample for the $\mathbf{H} \parallel \mathbf{I}$ configuration in fields up to 30 kOe. For 5, 80, and 150 K the dependences are very different from those observed in the case of $\mathbf{H} \perp \mathbf{I}$. In weak fields $\Delta\rho/\rho_0 \sim H^{0.42}$, $\Delta\rho/\rho_0 \sim H^{0.6}$, and $\Delta\rho/\rho_0 \sim H^{0.58}$, for temperatures of 5, 80, and 150 K, respectively, are observed. For 5 K, the power value is the lowest. As the temperature raises the range of magnetic fields in which the power dependence is observed increases. Then, as the field increases, the power dependence changes to a linear one. At 300 K, the dependence $\Delta\rho/\rho_0(H)$ for $\mathbf{H} \parallel \mathbf{I}$ is similar to that observed for $\mathbf{H} \perp \mathbf{I}$. Namely, there is the characteristic dependence $\Delta\rho/\rho_0 \sim \alpha_1 H + \beta_1 H^2$ in small magnetic fields (0–6 kOe), which turns into linear one with increasing field.

Discussion of the results

As we mentioned above, the sample $\text{Bi}_{95.69}\text{Mn}_{3.69}\text{Fe}_{0.62}$, which is investigated in this work, is a bismuth matrix with α -BiMn magnetic phase inclusions. The electrical conductivity in this sample is mainly due to current flow through the bismuth matrix, which is affected by the magnetism of α -BiMn magnetic phase inclusions, uniformly distributed in the sample volume. It would seem that the $\Delta\rho/\rho_0(H)$ dependences should be similar to those observed in pure bismuth. But the results of our experiments show that this is not the case. What can be the reason for the difference in the behavior of the magnetoresistance in pure bismuth and $\text{Bi}_{95.69}\text{Mn}_{3.69}\text{Fe}_{0.62}$?

First of all, the presence of magnetic inclusions of the α -BiMn phase can lead to additional scattering of charge carriers by magnons and the appearance of an additional contribution to the electrical resistance. In addition, it is well known that bismuth has several groups of charge carriers [16]. The Fermi surface of bismuth consists of one

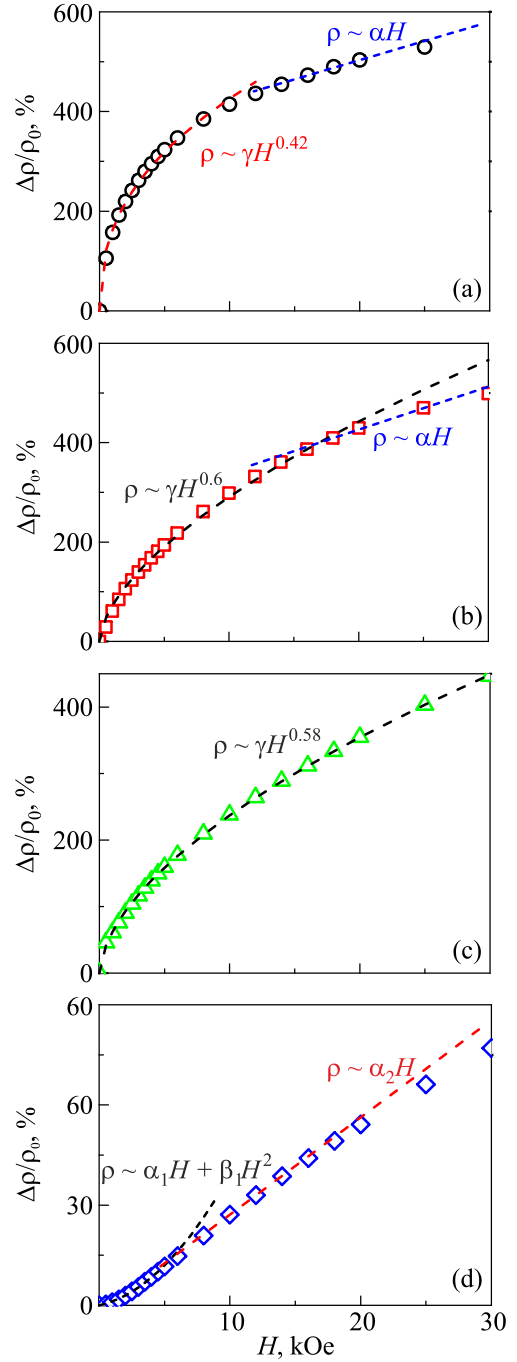


Fig. 4. (Color online) Magnetic-field dependences of the magnetoresistance $\Delta\rho/\rho_0 = (\rho_H - \rho_0)/\rho_0 \cdot 100\%$ of $\text{Bi}_{95.69}\text{Mn}_{3.69}\text{Fe}_{0.62}$ for the $\mathbf{H} \parallel \mathbf{I}$ at temperatures, K: 5 (a), 80 (b), 150 (c), and 300 (d).

hole pocket at the T-point and three electron pockets at the L-points in the first Brillouin zone of the rhombohedral cell [16]. These three equivalent electron pockets can be regarded as triply degenerate electron valleys in a zero magnetic field. Due to the strongly anisotropic shape of electron pockets, the degeneracy of the triple valley can be lifted in a rotating magnetic field [17, 18]. At L-points, bismuth has narrow gaps ($E_g \approx 15.3$ meV) between the conduction and the valence bands. The strong spin-orbit interaction ($\lambda \approx 1.8$ eV) leads to the fact that the electrons

at the L-point have almost linear dispersion dependence and can be considered as massive Dirac fermions [16, 19]. At the same time, the application of a magnetic field in certain directions can first reduce the gap at the L-points [18], and then cause level crossing as the field increases [20]. As the field increases further, the hole and electron sub-zones will shift in opposite directions and eventually a semimetal-semiconductor transition will occur [21, 22]. Thus, a magnetic field of a certain magnitude and direction can significantly affect the charge carriers by increasing or decreasing their concentration and mobility. The influence of internal magnetism can further complicate the situation by exerting additional influence on the carriers at the electron and hole pockets and leads to field dependences of the magnetoresistance of $\text{Bi}_{95.69}\text{Mn}_{3.69}\text{Fe}_{0.62}$ which are significantly different from those observed in pure bismuth. The polycrystallinity of the sample and intergranular scattering must also be taken into account. As a result, all these factors can lead to a difference in the magnetic-field dependences in our sample from the dependences observed in pure bismuth. It is also necessary to pay attention to the fact that according to the data of Ref. 23, in the α -BiMn phase below 100 K, the spin-reorientation transition in which manganese spins are oriented in space in a special way can be observed. Because of this, the form of magnetoresistance dependences in the case of $\text{Bi}_{95.69}\text{Mn}_{3.69}\text{Fe}_{0.62}$ on the magnetic field can differ when measured in the $\mathbf{H} \perp \mathbf{I}$ and $\mathbf{H} \parallel \mathbf{I}$ configurations.

It is worth dwelling in more detail on the behavior of the magnetic-field dependences of the magnetoresistance of $\text{Bi}_{95.69}\text{Mn}_{3.69}\text{Fe}_{0.62}$ in fields $H > 30$ kOe at liquid helium temperature. The $\Delta\rho/\rho_0(H)$ dependences at this temperature have a maximum in the fields ≈ 30 and ≈ 40 kOe, for the $\mathbf{H} \parallel \mathbf{I}$ and $\mathbf{H} \perp \mathbf{I}$ configurations, respectively. Earlier in the literature [24–26], a significant maximum was also observed in the magnetic field dependences of the longitudinal magnetoresistance of bismuth at approximately the same magnetic field values as for $\text{Bi}_{95.69}\text{Mn}_{3.69}\text{Fe}_{0.62}$. The maximum was associated with reaching the quantum limit, when only one Landau level remains below the Fermi level in the electron zone. In a semimetal, this leads to the “overflow” of charge carriers between the hole and electron zones. As a result, the concentration of electrons and holes increases and the electrical resistance decreases [25]. In Abrikosov’s work [27] a theoretical calculations were carried out for the limiting quantum case in the model of a multi-valley metal with an isotropic quadratic spectrum of charge carriers and with valleys spaced far apart in momentum space. According to this calculation, the longitudinal magnetoresistance ($\mathbf{H} \parallel \mathbf{I}$) in the fields greater than the maximum should decrease according to the H^{-1} law. Such dependence, indeed, takes place in pure bismuth [24–26]. Let’s see if it holds in our case. Figure 5 shows the magnetic-field dependences $\Delta\rho/\rho_0$ at temperatures of 5 K for the configurations $\mathbf{H} \perp \mathbf{I}$ and $\mathbf{H} \parallel \mathbf{I}$. It is clearly seen

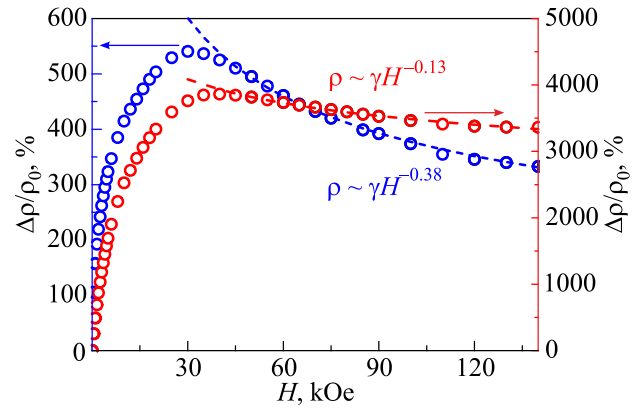


Fig. 5. (Color online) Magnetic-field dependences of magnetoresistance $\Delta\rho/\rho_0 = (\rho_H - \rho_0)/\rho_0 \cdot 100\%$ of $\text{Bi}_{95.69}\text{Mn}_{3.69}\text{Fe}_{0.62}$, for the $\mathbf{H} \perp \mathbf{I}$ (○) and $\mathbf{H} \parallel \mathbf{I}$ (○) at 5 K.

that in fields above the maximum $\Delta\rho/\rho_0 \sim H^{-0.38}$ and $\Delta\rho/\rho_0 \sim H^{-0.13}$, for the configuration $\mathbf{H} \parallel \mathbf{I}$ and $\mathbf{H} \perp \mathbf{I}$, respectively. The deviation of the magnetic-field dependence $\Delta\rho/\rho_0$ in the longitudinal field from $\Delta\rho/\rho_0 \sim H^{-1}$ can be due to the polycrystalline nature of the sample and the fact that for individual grains the orientation $\mathbf{H} \parallel \mathbf{I}$ is not fulfilled despite the texturization of the sample. In the case of a transverse field ($\mathbf{H} \perp \mathbf{I}$), according to [25, 27], the magnetoresistance should reach saturation when the quantum limit is obtained. In our case, instead of saturation, weak power dependence is observed, which can also be explained by the polycrystalline nature of the sample.

In general, in order to better understand the physical processes that affect the behavior of the anomalous magnetoresistance in $\text{Bi}_{95.69}\text{Mn}_{3.69}\text{Fe}_{0.62}$, additional studies are needed, including the measurements of the Hall effect, obtaining single-crystalline samples and studying their galvanomagnetic properties, as well as using ARPES to achieve information about the band structure in this multicomponent material. We will plan to carry out such studies in the future.

Conclusions

For the first time, the magnetic-field dependences of the electrical resistivity of the $\text{Bi}_{95.69}\text{Mn}_{3.69}\text{Fe}_{0.62}$ textured polycrystal have been studied in detail, for the $\mathbf{H} \perp \mathbf{I}$ and $\mathbf{H} \parallel \mathbf{I}$ configurations, in magnetic fields up to 140 kOe, and at temperatures of 5, 80, 150, and 300 K.

It has been shown that the $\Delta\rho/\rho_0(H)$ dependences differ significantly from those observed for pure bismuth.

It has been assumed that the main factor leading to the anomalous of the magnetoresistance behavior in $\text{Bi}_{95.69}\text{Mn}_{3.69}\text{Fe}_{0.62}$ is the influence of the internal magnetism of inclusions of the α -BiMn phase on the behavior of charge carriers (electrons and holes) in the bismuth matrix.

The maxima of $\Delta\rho/\rho_0(H)$ at $H \approx 30$ and ≈ 40 kOe have been found for $\mathbf{H} \parallel \mathbf{I}$ and $\mathbf{H} \perp \mathbf{I}$, respectively, which may be related to reaching the quantum limit in our samples.

Acknowledgments

The authors are grateful to Professor Yu. G. Naidyuk and DSc I. V. Zolocheskii for their useful discussions and remarks, which were helpful to the process of finalizing this article. The work was supported by the National Academy of Sciences of Ukraine within the F19-5 project. We acknowledge support from the European Federation of Academies of Sciences and Humanities (ALLEA) through Grant EFDS-FL1-32 (A.L.S.). A.L.S. also thanks the Division of Low Temperatures and Superconductivity, INTiBS Wrocław, Poland, for their hospitality. Work was partly funded by Research Council of Finland, project No. 343309.

1. L. A. Fal'kovskii, *Phys. Usp.* **11**, 1 (1968).
2. V. S. Edel'man, *Phys. Usp.* **20**, 819 (1977).
3. Om Prakash, Anil Kumar, A. Thamizhavel, and S. Ramakrishnan, *Science* **355**, 52 (2017).
4. P. Lejay, P. de Rango, A. Sulpice, B. Giordanengo, R. Tournier, R. Retoux, S. Deslandes, C. Michel, M. Hervieu, and B. Raveau, *Rev. Phys. Appl.* **24**, 485 (1989).
5. N. B. Brandt, E. A. Svistova, Yu. G. Kashirskii, and L. V. Lyn'ko, *Sov. Phys. JETP* **29**, 35 (1969).
6. D. Hsieh, D. Qian, L. Wray, Y. Xia, Y. S. Hor, R. J. Cava, and M. Z. Hasan, *Nature* **452**, 970 (2008).
7. Z. K. Liu, B. Zhou, Y. Zhang, Z. J. Wang, H. M. Weng, D. Prabhakaran, S.-K. Mo, Z. X. Shen, Z. Fang, X. Dai, Z. Hussain, and Y. L. Chen, *Science* **343**, 864 (2014).
8. Yong-Sheng Liu, Jin-Cang Zhang, Zhong-Ming Ren, Min An Gu, JingJing Yang, Shi-Xun Cao, and Zheng-Long Yang, *Chin. Phys. Lett.* **27**, 0975024-1 (2010).
9. N. V. Rama Rao, A. M. Gabay, and G. C. Hadjipanayis, *J. Phys. D* **46**, 062001 (2013).
10. A. V. Terekhov, A. L. Solovjov, A. I. Prokhvatilov, V. V. Meleshko, I. V. Zolocheskii, J. Cwik, A. Los, A. D. Shevchenko, O. M. Ivasishin, and Z. D. Kovalyuk, *East Eur. J. Phys.* **4**, 12 (2017).
11. A. V. Terekhov, K. Rogacki, A. L. Solovjov, A. N. Bludov, A. I. Prokhvatilov, V. V. Meleshko, I. V. Zolocheskii, E. V. Khristenko, J. Cwik, A. Los, A. D. Shevchenko, Z. D. Kovalyuk, and O. M. Ivasishin, *Fiz. Nizk. Temp.* **44**, 1475 (2018) [*Low Temp. Phys.* **44**, 1153 (2018)].
12. N. E. Alekseevskii and T. I. Kostina, *JETP* **21**, 807 (1965).
13. G. W. C. Kaye, *Proc. R. Soc. London A* **170**, 561 (1939).
14. N. B. Brandt, E. A. Svistova, and G. Kh. Tabieva, *JETP Lett.* **4**, 17 (1966).
15. P. Kapitza, *Proc. R. Soc. London A* **119**, 358 (1928).
16. Ayumu Iwasa, Akihiro Kondo, Shiro Kawachi, Kazuto Akiba, Yoshiki Nakanishi, Masahito Yoshizawa, Masashi Tokunaga, and Koichi Kindo, *Sci. Rep.* **9**, 1672 (2019).
17. Z. Zhu, A. Collaudin, B. Fauqué, W. Kang, and K. Behnia, *Nat. Phys.* **8**, 89 (2012).
18. Z. Zhu, J. Wang, H. Zuo, B. Fauqué, R. D. McDonald, Y. Fuseya, and K. Behnia, *Nat. Commun.* **8**, 15297 (2017).
19. P. A. Wolff, *J. Phys. Chem. Solids* **25**, 1057 (1964).
20. G. A. Baraff, *Phys. Rev.* **137**, A842 (1965).
21. K. Hiruma and N. Miura, *J. Phys. Soc. Jpn.* **52**, 2118 (1983).
22. N. Miura, K. Hiruma, G. Kido, and S. Chikazumi, *Phys. Rev. Lett.* **49**, 1339 (1982).
23. J. B. Yang, W. B. Yelon, W. J. James, Q. Cai, M. Kornecki, S. Roy, N. Ali, and Ph. l'Heritier, *J. Phys.: Condens. Matter* **14**, 6509 (2002).
24. V. V. Andrievskii, A. V. Butenko, Yu. F. Komnik, and V. Nikitin, *Sov. J. Low Temp. Phys.* **8**, 838 (1982).
25. A. V. Butenko and V. V. Andrievskii, *Sov. J. Low Temp. Phys.* **9**, 880 (1983).
26. R. Rosenbaum and J. Galibert, *Physica B: Condens. Matter* **346**, 291 (2004).
27. A. A. Abrikosov, *Sov. Phys. JETP* **29**, 746 (1969).

Особливості магнітоопору $\text{Bi}_{95.69}\text{Mn}_{3.69}\text{Fe}_{0.62}$ в магнітних полях до 140 кЕ

A. V. Terekhov, K. Rogacki, V. M. Yarovy,
V. B. Stepanov, Yu. A. Kolesnichenko,
A. D. Shevchenko, Z. D. Kovalyuk, E. Lähderanta,
A. L. Solovjov

Вперше досліджено магнітопольові залежності електроопору $\Delta\rho/\rho_0(H)$ текстурованого полікристала $\text{Bi}_{95.69}\text{Mn}_{3.69}\text{Fe}_{0.62}$ для конфігурацій $\mathbf{H} \perp \mathbf{I}$ та $\mathbf{H} \parallel \mathbf{I}$ за температур 5, 80, 150 та 300 К. Встановлено, що залежності $\Delta\rho/\rho_0(H)$ суттєво відрізняються від магнітопольових залежностей магнітоопору для чистого вісмуту внаслідок впливу внутрішнього магнетизму включень α - BiMn фази на поведінку носіїв заряду в матриці вісмуту. Виявлено максимуми $\Delta\rho/\rho_0(H)$ при $H \approx 30$ та ≈ 40 кЕ для відповідно поздовжнього і поперечного магнітоопорів, які можуть бути пов'язані з досягненням квантової межі.

Ключові слова: магнітопольові залежності електроопору, текстурований полікристал α - BiMn фаза, вісмут, квантова межа.